Conversion and Interaction Point Simulation of a $\gamma\gamma$ Collider at the NLC

T. Takahashi[1] * K. Yokoya[2] V. Telnov[3] M. Xie[4] and K-J. Kim[4]
[1]*Department of Physics, Hiroshima university Higashi-Hiroshima, 739, Japan*
[2]*KEK-National Laboratory for High Energy Physics, 1-1 Oho Tsukuba, 305, Japan*
[3]*Institute of Nuclear Physics 630090, Novosibirsk, Russian Federation*
[4]*Lawrence Berkeley National Laboratory, Berkeley, CA 94720, USA*

ABSTRACT

We study the performance of a $\gamma\gamma$ collider by Monte Carlo simulations. The luminosity distribution are calculated taking into account the generation of high energy photons by Compton backscattering at the conversion point and the successive beam-beam collision at the interaction point. The results of three separate simulation codes are compared and found to be in a reasonable agreement with each other.

I. INTRODUCTION

The $\gamma\gamma$ collision is one of the possible experimental programs at the second interaction region in the Next Linear Collider (NLC). The idea of generating high energy photons by backscattered Compton photons has been studied in papers [1, 2, 3, 4, 5] and were summarized in [6].

Physics opportunities in $\gamma\gamma$ collisions at a few hundreds GeV are rich [6, 7, 8, 9], some of which are:

- Study of two photon decay width of Higgs particle. Since Higgs decays to two photons through loops of charged particles, the decay width is sensitive to the number of heavy charged particles and can be a signal of new physics beyond the standard model.
- Because of large cross section of W pair production, $\gamma\gamma$ collider can be a W factory and is useful for study of the property of Ws, such as anomalous coupling.

The scheme of a $\gamma\gamma$ collider is illustrated in fig.1. In $\gamma\gamma$ colliders, high energy photons are created by Compton scattering between intense laser and high energy electron beams. The energy spectrum and polarization of the scattered high energy photons are controlled by polarization of the laser and of the electron beams which can be chosen to fit various physical requirements.

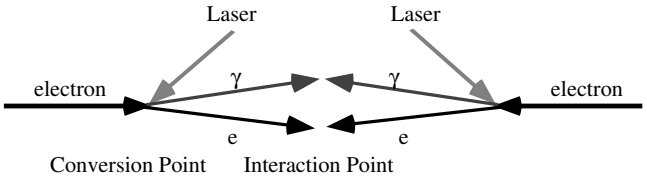

Figure 1: A Schematic view of a photon linear collider.

In order to achieve high luminosity, almost all electrons in a bunch must meet laser photons at the conversion point. In this environment, an electron suffers from multiple Compton scattering in a single laser pulse which results in low energy tail in the electron as well as in the photon spectra. The density of electrons and intensity of lasers, which change the probability of Compton scattering in an electron-laser collision, are of course not constant in space-time and must be calculated from parameters of the electron and laser beams. Since it is impossible by an analytic method to calculate the photon spectrum and luminosity distribution taking account of these multiple Compton scattering in a realistic condition, we have to rely on Monte Carlo simulations.

After the photon generation at the conversion point, spent electrons as well as high energy photons are transported to the interaction region. To get a clear $\gamma\gamma$ collision, the spent electrons from the conversion point need to be swept away from the interaction region by an external magnetic field in the transported region. Since, as described later, typical size and field strength of the magnet is in the order of cm and Tesla, and the magnet must not interfere with precise measurement of vertex position of b quark decay, it is not trivial if the magnet can be installed in real experiments. In the case without the sweeping magnet, all particles from the conversion point collide with particles from the opposite beam at the interaction point. The beamstrahlung from the beam-beam interaction changes the shape of luminosity spectra of the $\gamma\gamma$ collision as well as some amount of $e^-e^-$and $e^-\gamma$ collision occured at the interaction point. Therefore, detailed knowledge of the beam-beam interaction is necessary for determination of the initial state in physics analysis and for estimation of backgrounds to the detector.

For e^+e^-collider, a simulation program for beam-beam interaction including incoherent production of low energy electron-positron pairs was developed [10] and has been used for luminosity and detector background estimation [11, 12]. A similar kind of simulation is necessary for the interaction region of a $\gamma\gamma$ collider. However, simulation is more complicated than that of e^+e^-colliders since the simulation has to take account of photons as well as electrons from the conversion point, and energy and angular divergence of the particles are widely spread compared with the e^+e^-collider. To meet these requirements, simulation codes has been developed.

In this paper, we report the results of a simulation of the conversion and the interaction region in a 0.5 TeV $\gamma\gamma$ collider as an option of the NLC. We also report comparison of results of independent simulations to see the reliability of the simulation.

* corresponding author. e-mail address, tohrut@kekux1.kek.jp

II. PARAMETERS OF THE $\gamma\gamma$ COLLIDER

A. Electron Beam

A set of reference parameters of a $\gamma\gamma$ collider option of the NLC is summarized in Table 1. The detail of the parameters choice is described elsewhere [11].

Table I: Parameters for a photon-photon collider

Electron beam parameters	
Beam energy	$\mathcal{E}_b$=250 GeV
Particles per bunch	$N = 0.65\times 10^{10}$
Repetition rate	$f_{rep} = 180$ Hz
Number of bunches per pulse	$n_b = 90$
Bunch length	σ_z=100 μm
Bunch sizes (C.P.)	σ_x=718 nm
	σ_y=91 nm
Bunch sizes (I.P.)	σ_x=71 nm
	σ_y=9.1 nm
Beta functions (I.P.)	β_x=0.5 mm
	β_y=0.5 mm
Emittance	$\gamma\varepsilon_x$=5.0 $\times$ 10^{-6} m·r
	$\gamma\varepsilon_y$=8.0 $\times$ 10^{-8} m·r
C.P-I.P distance	b=5 mm
Laser parameters	
Wave length	$\lambda_L = 1.054\ \mu$m
Pulse energy	1 J
Pulse length	$\sigma_z^L = 0.23$ mm
Peak power density	1×10^{18} W/ cm^2
Repetition rate	180×90 Hz
r.m.s spot size	$\sigma_r^L = 2.9\ \mu$m

Since the luminosity of photon-photon colliders is approximately proportional to the geometric luminosity and, unlike e^+e^-colliders, there is no strong beamstrahlung at the interaction, the higher geometric luminosity is preferable. Since the angular divergence of backscattered high energy photons is $\approx 1/\gamma$, where γ is the electron energy divided by its rest mass, the smaller of the electron beam size, i.e. the vertical size, is determined by relation

$$\sigma_y \approx b/\gamma$$

which could be larger than the e^+e^-collider case. However, thanks to the absence of beamstrahlung, the horizontal beam size in the $\gamma\gamma$ collider can be much smaller than the e^+e^-collider [6]. In fact, the horizontal beam size in the NLC $\gamma\gamma$ collider is limited by beam emittance while it is limited by beam-beam interaction in the e^+e^-collider. With $\beta_x = 0.5$ mm, geometric luminosity of e^-e^-collision is $8.7 \times 10^{33}\ \mathrm{cm}^{-2}s^{-1}$, which is larger than the typical NLC e^+e^-collider ($4.3 \times 10^{33}\ \mathrm{cm}^{-2}s^{-1}$) [11].

B. Laser Parameters

The goal for choosing laser parameters is to obtain conversion efficiency as high as possible while keeping the achievable level of laser power and nonlinear QED effect at a tolerable level.

The reference laser parameters are chosen so that conversion efficiency of the incoming electrons in a laser pulse is about 0.65. It is achieved with a peak laser power of 0.5 TW, and the peak laser power density at the focus point is about $10^{18}\ \mathrm{W/cm^2}$. The nonlinear QED parameter with this power density is:

$$\xi^2 = \left(\frac{eE}{\omega mc}\right)^2 \approx 0.4\left[\frac{I}{10^{18}\ \mathrm{W/cm^2}}\right]\left[\frac{\lambda_L}{1.054\ \mu\mathrm{m}}\right]^2 \approx 0.4$$

where e, E, ω, m, c, I and λ_L are electric charge, strength of laser field, laser photon energy, electron mass, speed of light, laser intensity and laser wavelength respectively.

With this set of electron and laser parameters, the Compton kinematic parameter is $x = 4\mathcal{E}_b\omega/m_e^2 = 4.47$, and the maximum photon energy $\mathcal{E}_{max}$ in the linear Compton limit is

$$\mathcal{E}_{max} = \frac{x}{x+1}\mathcal{E}_b \approx 200\ \mathrm{GeV}$$

which is about 80% of the original beam energy.

As described in the previous section, the treatment of spent electrons coming out of the conversion region is one of the important issues to be discussed in $\gamma\gamma$ colliders. In the reference parameter, we chose the $1\sigma_y$ offset collision scheme without the sweeping magnet; i.e., two electron beams have vertical $1\sigma_y$ offset at the interaction point to reduce the effect of beam-beam interaction while keeping the reduction of $\gamma\gamma$ luminosity at a tolerable amount.

III. CODE DEVELOPMENT

Since processes in the conversion and interaction regions of $\gamma\gamma$ colliders are complex and diverse, it is necessary to use simulation codes to estimate luminosities and detector backgrounds. Processes and phenomena which should be taken care of at the conversion region are:

- Compton and Breit-Wheeler processes including the nonlinear QED effect.
- The polarization of the electron and laser beam. Circular (laser)/longitudinal (electron) as well as linear (laser)/transverse (electron) polarization should be taken into account.
- Diffraction of lasers and electron transportation according to given beam parameters.
- Multiple Compton scattering of a electron in a laser pulse.

The electrons and photons coming out of the conversion region are transported to the interaction region. During the transportation, electrons may be swept by an external magnetic field. The simulation should include the external field and the synchrotron radiation. All particles transported to the interaction region meet the particles from the opposite beam. The beam-beam interactions which should be included in the simulation are:

- Disruption and beamstrahlung.
- Incoherent electron positron pair creation by Breit-Wheeler, Bethe-Heitler and Landau-Lifshitz processes.

- Coherent pair creation.

To meet the requirement, a program called CAIN has been developed. Details of code development are described elsewhere [13, 14]. Version 1.0 of CAIN (CAIN1.0) which can be applied for general e^+e^-, $\gamma\gamma$, $e^-\gamma$ and e^-e^-types of linear colliders has been developed. In the conversion and transportation region, CAIN1.0 meets all requirements listed above except the treatment of polarization in nonlinear Compton and Breit-Wheeler processes. In nonlinear QED calculations, electrons and laser photons are assumed to be in an eigenstate of helicity, i.e., linear polarization of the laser is not taken into account. It is a point to be improved upon in the future, since linear polarization of the laser (and high energy photons as a result) is useful, for example, for the study of CP state of Higgs particle [15]. It should be noted that linear Compton scattering was installed in CAIN1.0 as well, which can treat polarization of photons and electrons in the most general way. For the simulation of the interaction point, a modified version of a simulation code for e^+e^-colliders, ABELMOD [10], is used. ABELMOD includes beam disruption, beamstrahlung and incoherent pair creation, but does not include coherent pair creation. Since the initial state of ABELMOD is, by definition, electron and position beams, it has been modified to accept photons from the conversion and the transportation region for $\gamma\gamma$ colliders application. A more sophisticated version, CAIN2.0, is under development by one of the authors (K.Y). It is newly developed and does not share any code between ABELMOD, while CAIN1.0 used many subroutines even in the conversion region. The physical process treated in the simulation is the same as CAIN1.0, but CAIN2.0 includes the coherent pairs in the interaction region.

Independent of the CAIN project, a simulation code was developed by Telnov [11]. Physical processes in Telnov's simulation are almost the same as CAINs, but there are a few additional assumption:

- The conversion efficiency in Compton scattering is fixed at a value given by hand and a laser pulse is simulated as a photon target of a certain thickness.
- The direction of the helicity of the electron and the laser photon is fixed and does not flip in the scattering.
- Nonlinear QED effect is not included.

In spite of the assumption, as described in next section, these effects are not significant in typical $\gamma\gamma$ collider parameters and the results are consistent with CAIN simulation.

IV. SIMULATION

The energy spectrums of Compton scattered photons are plotted in fig.2 for linear and nonlinear QED calculations by CAIN1.0. In the simulation, it is assumed that the laser beam is 100% circularly polarized and the electron beam is 100% longitudinally polarized. The combination of the polarization of the laser (P_γ) and the electron (P_e) beams is chosen as $P_\gamma P_e = -1$, which produces a relatively narrow peak at the high energy edge. Comparing nonlinear and linear Compton spectra,

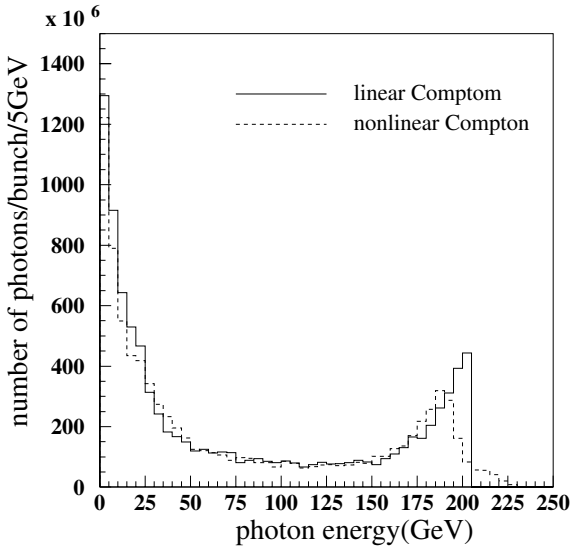

Figure 2: Simulated photon energy spectrum from the Compton conversion point without (solid) and with (dashed) nonlinear QED effect.

the maximum energy of photons in nonlinear processes exceeds $\mathcal{E}_{max} = x\mathcal{E}_b/(x+1) \approx 200$ GeV due to multiple laser photon absorption. It is also seen that the high energy peak of about 200 GeV in linear Compton is shifted to a lower value in the nonlinear spectrum. This is another effect of nonlinear interaction, i.e., increasing effective electron mass. The peak energy is consistent with the expected value,

$$\mathcal{E}_{max} = \frac{x\mathcal{E}_b}{x+\xi^2+1} \approx 190 \text{ GeV}.$$

A differential luminosity spectrum is shown in fig.3. In $L_{\gamma\gamma}$ distribution, the high c.m.s energy part is made by the collision of Compton photons. In the low energy region, a large low energy tail is seen in the spectrum. The source of the tail is beamstrahlung, i.e., the collision of beamstrahlung photons with beamstrahlung and Compton photons. In the figure, results from the three (CAIN1.0, CAIN2.0 and Telnov's) calculations are plotted. Since CAIN2.0 and CAIN1.0 are essentially same program, the results agree well. A Difference seen between CAINs and the Telnov's calculation mainly comes from nonlinear QED effect since Telnov's calculation does not include the effect. With the nonlinear calculation, high energy peak is shifted to lower value due to the shift in Compton photon spectrum, and the peak becames broader than the linear Compton case. The $\gamma\gamma$ luminosity in the high energy region is about 9% of geometric luminosity and 11% in linear Compton calculation because of broadness of the high energy peak. The nonlin-

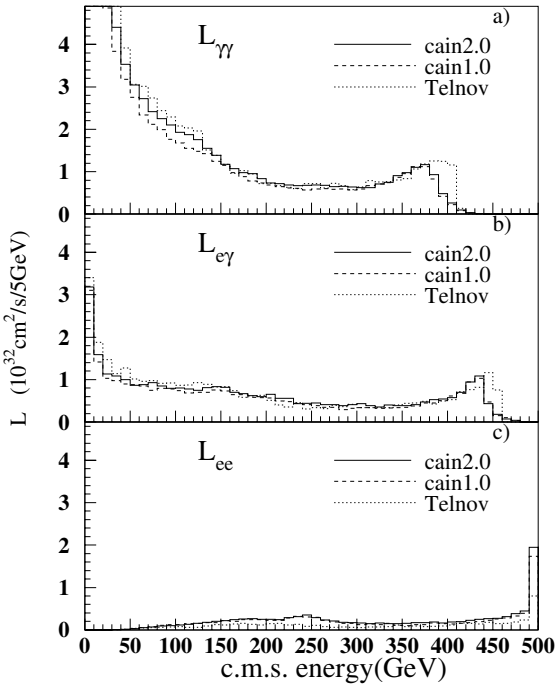

Figure 3: Simulated luminosity distribution of a $\gamma\gamma$ collider for $\gamma\gamma$ (a) $e^-\gamma$ (b) e^-e^-(c) luminosity distribution. Solid, dashed and dots line corresponds to CAIN10, CAIN20 and Telnov's simulation respectively.

ear effect lowers the peak energy and broadens the peak, however, with this set of parameters $\xi^2 = 0.4$, the effect is not very significant and is at a tolerable level. Obtained luminosities are summarized in Table 2 for total and high center of mass energy, $z = W_{\gamma\gamma}/2\mathcal{E}_b > 0.65$, region. In the table, calculation by CAIN2.0 without nonlinear QED effect is also shown as a reference and agrees with Telnov's calculation.

Table II: Summary of the luminosity

CAIN Simulation	linear(nonlinear)QED
$L_{\gamma\gamma}$	0.97(0.99) L_{geom}
	0.09(0.11) L_{geom} ($z > 0.65$)
$L_{e\gamma}$	0.75(0.76) L_{geom}
	0.17(0.17) L_{geom} ($z > 0.65$)
L_{ee}	0.13(0.12) L_{geom}
	0.07(0.06) L_{geom} ($z > 0.65$)
Telnov Simulation	linear QED
$L_{\gamma\gamma}$	1.09 L_{geom}
	0.11 L_{geom} ($z > 0.65$)
$L_{e\gamma}$	0.78 L_{geom}
	0.19 L_{geom} ($z > 0.65$)
L_{ee}	0.11 L_{geom}
	0.06 L_{geom} ($z > 0.65$)

The effect of beam-beam interaction at the interaction points is beamstrahlung as well as disruption. The disruption angle due to coulomb force of the opposite beams can be estimated as [16]:

$$\theta_d = \frac{2Nr_e}{\gamma\sigma_x}$$

where r_e is the electron classical radius. However this formula can be applied to the case that $\theta_d < 4\sigma_x/\sigma_z$, which is approximately 10 mr in the reference parameters. In the case of large disruption, the angle can be estimated by [4]:

$$\theta \approx \sqrt{\frac{4\pi Nr_e}{\gamma\sigma_z}}.$$

Due to the multiple Compton scattering in the conversion region, the electron energy can be as low as a few GeV, and the disruption angle is about 15 mr. In order to clear the quadrupole magnet, an extra 10 mr crossing angle is required compared with the e^+e^-collider. For a detailed design of the interaction region, taking these low energy electrons into account, a simulation study is necessary. However, simulation of 10^3 out of 10^{10} particles requires a sophisticated treatment of the weight of the particle which is only available in CAIN2.0.

Fig.4 shows the luminosity distribution with the sweeping magnet simulated by CAIN1.0.

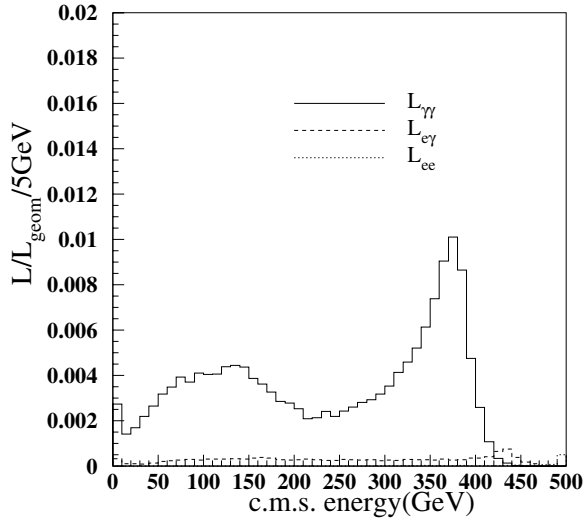

Figure 4: Simulated luminosity distribution for the case with sweeping magnet. The length and strength of magnetic field are 1 cm and 1 Tesla in horizontal direction. Solid, dashed and dots line corresponds to $\gamma\gamma$, $e^-\gamma$ and e^-e^-luminosity distribution respectively.

The electron and laser beam parameters are the same as in the previous section except the distance between the conversion and interaction points. For realistic installation of a sweeping magnet, the distance is enlarged to 1 cm from 5 mm. The magnetic field is assumed to be 1 Tesla, which takes a 250 GeV electron beam 60 nm from the interaction point.

Since the conversion point is shifted to $b = 1$ cm, the spatial spread by angular divergence, $1/\gamma \times 1\ \mathrm{cm} \approx 20\ \mathrm{nm}$, which is twice as larger as the $b = 5$ mm case. For the reference parameters, the vertical photon beam size is dominated by the angular divergence of the scattered photons, while horizontal size is fixed by the electron beam parameter. So the $\gamma\gamma$ luminosity is expected to be reduced by a factor of 2 by the shift of the conversion point. In the meantime, it is not necessary for the $1\sigma_y$ offset, since there is no hard electron collision at the interaction point, and the $\gamma\gamma$ luminosity increases some amount compared with the $1\sigma_y$ offset case. Eventually, by the CAIN1.0 simulation with nonlinear QED effect, the $\gamma\gamma$ luminosity for $z > 0.65$ is slightly down to 6% of the geometric luminosity, while it is 9% in the case without sweeping magnet.

With the sweeping magnet, the beam-beam interaction at the interaction region can be ignored and there is no beam disruption in the horizontal direction. So the beam crossing angle can be the same as e^+e^-colliders. It should be remarked that this is not valid for beams with halo, and additional study is needed in this case.

V. SUMMARY

We studied processes in the conversion and interaction regions in a 0.5 TeV $\gamma\gamma$ collider based on the NLC. The high energy photon spectra and luminosity were calculated with a reference parameter and we found that $\gamma\gamma$ luminosity in high energy ($z = w_{\gamma\gamma}/2\mathcal{E}_b$) is about 10% of geometric luminosity. Three simulation codes were used with the same set of electron and laser beam parameters and gave us consistent results for luminosity distributions of $e^-\gamma$, e^-e^-as well as $\gamma\gamma$ collision.

We now have a reliable method of stuying the conversion and interaction regions of $\gamma\gamma$ and $e^-\gamma$ colliders. More detailed study such as design of the interaction region, detector background and optimization of the machine parameters are in progress.

VI. ACKNOWLEDGMENTS

We would like to thank Drs. P. Chen, M. Ronan, A. Spitkovsky and T. Ohgaki for providing us the CAIN program. We also thank all members of NLC $\gamma\gamma$ working group for useful discussion. One of the autos (T.T) thanks Prof. I. Endo for giving him a chance to stay at SLAC and to work on this subject.

VII. REFERENCES

[1] I. Ginzburg, G. Kotkin, V. Serbo, V. Telnov, *Pizma ZhETF* 34 (1981) 514; *JETP Lett.* 34 (1982) 491; *Prep. INP* 81-50, Novosibirsk.

[2] I. Ginzburg, G. Kotkin, V. Serbo, V. Telnov, *Nucl. Instr. Meth.* 205 (1983) 47; *Prep. INP* 81-92, Novosibirsk.

[3] I. Ginzburg, G. Kotkin, V. Serbo, V. Telnov, *Nucl. Instr. Meth.* 219 (1984) 5.

[4] V. Telnov, *Nucl. Instr. Meth* A294 (1990) 72.

[5] V. Telnov, *Proc. of Workshop on Gamma-Gamma Colliders*, Berkeley, CA, USA, 1994, published in *Nucl. Instr. Meth.* A355 (1995) 3.

[6] *Proc. of Workshop on Gamma-Gamma Colliders*, Berkeley, CA, USA, 1994, published in *Nucl. Instr. Meth.* A355 (1995).

[7] *Proc. of INS Workshop 'Physics of e^+e^-, $e^-\gamma$, and $\gamma\gamma$ collisions at Linear Accelerators'* Tokyo, Japan, 1994 published in INS-J-181 (1995).

[8] M. Baillargeon, G. Belanger, F. Boudjema, ENSLAPP-A-473/94.

[9] T. Takahashi Hiroshima university preprint, HUPD-9526.

[10] T. Tauchi, K. Yokoya and P. Chen, *Part. Acc.* 41 (1993) 29.

[11] *Zeroth-Order Design Report for the Next Linear Colliders* SLAC-474 (1996).

[12] *JLC-I* KEK-Report 92-16 (1992).

[13] P. Chen, G. Horton-Smith, T. Ohgaki, A.W. Weidemann, K. Yokoya, *Nucl. Instr. Meth.* **A335** (1995) 107.

[14] P. Chen, T. Ohgaki, A. Spitkovsky, T. Takahashi, K. Yokoya, in preparation

[15] B. Grzadkowski and J.F. Gunion, *Phys. Lett.* **B294** (1992) 361 M. Kramer, J. Kuhn, M.L. Stong, P.M. Zerwas, *Z. Phys.* **C64** (1994) 21

[16] R. Hollebeek, *Nucl. Instr. Meth.* **184** (1981) 333